Calibrated brightfield-based imaging for measuring intracellular protein concentration

Nathan J Mudrak, Priyanka S Rana, Michael A Model[1]

Department of Biological Sciences, Kent State University, Kent, OH 44242 USA
[1]Corresponding author: mmodel@kent.edu, 1-330-672-0774

Abstract

Intracellular protein concentration is an essential cell characteristic which manifests itself through the refractive index. The latter can be measured from two or more mutually defocused brightfield images analyzed using the TIE (transport-of-intensity equation). In practice, however, TIE does not always achieve quantitatively accurate results on biological cells. Therefore, we have developed a calibration procedure that involves successive imaging of cells in solutions containing different amounts of added protein. This allows one to directly relate the output of TIE (T) to intracellular protein concentration C (g/l). The resultant relationship has a simple form: $C \approx 1.0(T/V)$, where V is the cell volume (μm^3) and 1.0 is an empirical coefficient. We used calibrated TIE imaging to characterize the regulatory volume increase (RVI) in adherent HeLa cells placed in a hyperosmotic solution. We found that while no RVI occurs over the first 30-60 min, the protein concentration fully recovers after 20 h. Furthermore, interpretation of such long experiments may depend on whether protein concentration varies significantly throughout the cell cycle. Our data on HeLa, MDCK and DU145 cells indicate that it remains relatively stable.

Keywords: transport-of-intensity equation, intracellular water, regulatory volume increase, volume set point, transmission-through-dye imaging.

Introduction

Several decades of research have revealed the active role of cell volume in many biological processes (Hoffmann et al, 2009). Not surprisingly, the majority of studies of cell volume regulation have been based on measurements of none other than cell volume. It is important to keep in mind, however, that the cell volume comprises two quite different entities: 15-30% of the volume is occupied by membrane-impermeant organic macromolecules (of which protein typically makes up more than a half (Heijnen, 2010), while the rest of the volume is occupied by water with dissolved salts. In studying rapid volume changes, such as in response to osmolarity of the medium, it is usually safe to assume that those are caused entirely by redistribution of water. However, in slower processes, the origin of volume changes is not so clear. For example, cell growth and enlargement may result from both protein and water accumulation, and not necessarily in the same proportion. Likewise, shrinkage during apoptotic cell death may result not only from water expulsion and but also from cell fragmentation, and without evaluating the contribution of each, one may come to erroneous conclusions. Clearly, in some cases, the best approach would be to measure cell volume and cell water (or an equivalent pair of parameters) separately.

Cell protein concentration can be determined from the fact that it is related to the average refractive index of the cell. For most proteins, the refractive index increment is close to 0.19 ml/g (Liu et al, 2016; Theisen et al, 2000; Zhao et al, 2011), and for other common biological molecules it is either similar or slightly smaller (Liu et al, 2016; Theisen et al, 2000). Thus, if the refractive index difference between a cell and a low-protein medium is $n - n_o = \Delta n$, cell protein concentration can be estimated as

$$C(g/ml) \approx 5\Delta n \tag{1}$$

Cell refractive index has been measured using various experimental approaches (Liu et al, 2016), including quantitative phase microscopy. The latter term refers to a group of techniques that measure the phase delay of the light wave passing through a sample. If cell thickness or cell volume are known independently, the average refractive index of the cell can be found. The method of phase restoration based on the transport-of-intensity equation (TIE) is particularly attractive due to its simple technical realization, requiring nothing beyond a standard brightfield microscope capable of precise vertical movement.

TIE quantitatively expresses the well-known fact that visibility of refractive index-mismatched objects changes with defocusing. Specifically, it relates the gradient of intensity I in the axial direction z to the phase delay φ:

$$\frac{\partial I_{xy}}{\partial z} = -\frac{\lambda}{2\pi}\nabla \cdot \left(I\nabla\varphi_{xy}\right) \tag{2}$$

In practice, one collects at least two brightfield images I_1 and I_2 at different distances to the sample, and the difference between them is used to approximate the gradient $\frac{\partial I}{\partial z}$ (Ishizuka and Allman, 2005).

In spite of abundant literature on numerical methods of solving the TIE equation, there is a noticeable paucity of quantitative data on biological objects. Although various published images of biological cells look very believable (Barone-Nugent et al, 2002; Jingshan et al, 2014), the numerical accuracy of TIE with biological objects has scarcely been demonstrated. Measurements on erythrocytes have produced correct values in one work (Phillips et al, 2012) but not in another one (Gorthi and Schonbrun, 2012).

The measured refractive index of $\Delta n = 0.023$ for smooth muscle cells (Curl et al, 2005) corresponds to C ≈ 0.13 g/ml (according to Eq. (1),) which is significantly smaller than the numbers for similar cells obtained by other methods (Arvill et al, 1969; Fulton, 1982; Jones, 1982).

We too have previously attempted TIE on cultured cells (Model and Schonbrun, 2013). Qualitatively, the results were very consistent, and the water content in healthy HeLa cells was close to 85%, which is a reasonable number. However, it appears that the focus drive on our microscope was miscalibrated, and the good match was purely fortuitous; later we were unable to reproduce our own results on other microscopes and instead kept getting values for intracellular water over 90%.

In view of good qualitative but uncertain quantitative results, we propose a different approach to TIE imaging. Instead of interpreting the output T(x,y) of the TIE equation as the phase delay $\varphi(x,y)$, we make allowance for possible experimental or computational errors and postulate that T is not necessarily equal, but only proportional to the phase delay:

$$T(x,y) \propto \varphi(x,y)$$

We then calibrate the system by placing cells in solutions of bovine serum albumin (BSA) with varying concentrations C_0 to find the empirical coefficient of proportionality q_p:

$$T/V = q_p(C - C_o) \tag{3}$$

In this equation and for the rest of the paper, T stands for the integral value computed over the entire cell area and V is the cell volume. The latter can be measured by transmission-through-dye (TTD) imaging (see below), which is fully compatible with TIE.

If desired, calibration can be easily converted into units of intracellular water (as the volume fraction W):

$$T/V = q_w(W_o - W) \tag{4}$$

or into refractive index difference:

$$T/V = q_n(n - n_o) \tag{5}$$

Interpretation of intracellular protein or water data in experiments that involve prolonged cell treatments would depend on whether these parameters remain stable throughout the cell cycle. For example, if water were found to naturally accumulate in cells during mitosis and a particular treatment prevented cell division, the results could be easily skewed by accumulation of cells at the M phase. Since data from the literature have been controversial (Anderson et al, 1970; Beall et al, 1976; Bryan et al, 2010; Loken and Kubitschek, 1984; Rao et al, 1982; Zucker et al, 1979), we investigated cell water/protein content during cell cycle in three different cell types (HeLa, DU145 and MDCK) and concluded that in these cells, there is no significant variation of protein concentration throughout the cycle.

In the third part of the work, we present one example of the utility of TIE. In many cell types, the initial volume response to a change in external osmolarity is followed by a full or partial return to the initial

volume known as the regulatory volume increase (RVI) or regulatory volume decrease (RVD). The majority of data on RVI or RVD have been collected within a relatively brief period following the osmolarity change, presumably to avoid complications resulting from cell growth. By measuring the intensive parameter of protein/water concentration, rather than the extensive parameter of volume, this complication is avoided and a new aspect of cell behavior can be revealed.

Methods

Cell culture. HeLa, Madin-Darby canine kidney (MDCK) and human prostate cancer cells DU145 (American Type Culture Collection, Manassas, VA) were grown on coverslips in Dulbecco's Modified Eagle Medium (DMEM, Lonza) with 10% fetal bovine serum and antibiotics. For microscopic observation, the medium was replaced with one containing additionally 6-7 mg/ml Acid Blue 9 (AB9; TCI America, Portland, OR), and coverslips were placed upside down on slides over small spots of silicon grease to keep them above the slide surface at a distance that could be adjusted by applying light pressure. As explained below, the purpose of AB9 is to enable volume measurements by TTD; the dye at this concentration does not have any noticeable effects on cell viability and functioning (Gregg et al, 2010). In prolonged experiments, drying of the liquid was prevented by keeping slides in closed Petri dishes on lightly wetted paper towels; immediately before observation, the solution under the coverslips was replaced with a bolus of fresh medium.

Image acquisition. The samples were observed on an Olympus IX81 inverted microscope using 20x/0.7 or 10x/0.4 Planapo objectives and a NA0.55 condenser set for Köhler illumination. Images were captured with a SensiCam QE CCD camera (Cooke, Romulus, MI). Illumination was delivered to the samples either through a 485/10 bandpass (Omega Optical, Brattleboro, VT) for brightfield images required for TIE or through a 630/10 filter (Andover, Salem, NH) for volume measurement. For DNA quantification, cells were stained with 10 μg/ml of Hoechst 33258 (Sigma-Aldrich, St. Louis, MO) for 5-10 min and imaged in epifluorescence through a DAPI filter set. To take account of spatial variability of the field brightness, a uniform fluorescent field was prepared using 30% sodium fluorescein (Sigma-Aldrich, St. Louis, MO) (Model and Burkhardt, 2001; Model, 2014). Original fluorescence images of the sample R were corrected by the image of the uniform sample S as

$$\text{Corrected}_{ij} = \frac{R_{ij}}{S_{ij}} \bar{S}$$

where $\bar{S}$ is the average gray level of image S and the subscripts ij indicate that the division is performed on a pixel-by-pixel basis.

Volume measurements. The TTD method for volume measurement is based on absorption of transmitted light at 630 nm by extracellular dye AB9. This cell-impermeant is displaced by the cells, making them appear brighter against the dark background (Model, 2012; Model, 2015). Cell volume V is calculated from a single transmission image as

$$V = \sum_A h_{ij} - A\bar{h}_{bkg}$$

$$h_{ij} = \frac{\ln I_{ij}}{\alpha}$$

Here I_{ij} is the pixel gray value (corrected for the dark level of the camera), α is the absorption coefficient of the medium at 630 nm (measured as described previously (Model et al, 2008)), A is the cell area and h_{ij} is the logarithmic intensity, whose difference between the cell and the background average $\bar{h}_{bkg}$ represents the local cell thickness.

TIE analysis. TIE analysis is based on the estimation of the vertical gradient of image intensity from at least two mutually defocused brightfield images I_1 and I_2. Preliminary experiments were conducted to find the conditions that produced the most consistent data and low sensitivity to the choice of focal planes. Thus, image I_1 was focused on the surface of a coverslip and image I_2 was obtained by moving the objective 5 µm toward the sample (there is, indeed, a theoretical justification for focusing into the sample rather than away from the sample (Khitrin and Model, submitted)). To reduce granularity, each plane was imaged 20 times, and the averaged images were used.

TIE processing was performed on MATLAB R2012b (MathWorks, Natick, MA) using the code of Gorthi and Schonbrun (2012). TIE image quality is greatly improved when the background levels in both images are equal within no more than one gray scale unit; because our TIE code does not automatically equalize the intensities, we manually added or subtracted a small number from I_1 or I_2. For example, if the average background pixel intensity is 2500 for I_1 and 2510 for I_2, then adding 10 units to I_1 flattens the background and makes the analysis more reliable. Following other authors, the nominal step size (5 µm) was used in the computations without correction for axial elongation due to refractive index mismatch (Carlsson, 1991; Visser et al, 1992).

The rest of the analysis was done with ImageJ (http://imagej.nih.gov/ij/). A contour with area A was drawn around the cell on a TIE image, and the average gray level $\bar{T}_{cell}$ was determined; next, the average background level $\bar{T}_{bkg}$ was measured on a 3-µm band adjacent to the original contour, and the integral value over the cell was calculated as $T = A(\bar{T}_{cell} - \bar{T}_{bkg})$. A similar method of analysis was used for cell volume and for DNA quantification.

Calibration of TIE. All buffers used in the calibration experiments were based on Dulbecco's Phosphate-Buffered saline with added 1 µM $CaCl_2$, 1 µM $MgCl_2$ and 7 mg/ml AB9. The buffers also contained BSA (Amresco, Solon, OH) in concentrations ranging from 0 to 0.27 g/L and were made isosmotic (although the latter was not essential) by adding water or NaCl; the final osmolality measured on a vapor pressure osmometer Vapro 5520 (Wescor, Logan, UT) was 308 mOsm. Coverslips with attached live HeLa cells were placed onto a slide as described earlier and imaged consecutively in at least two buffers with different BSA concentrations. The cell volume and the output of TIE (T) were determined for every set of images. The protein-based coefficient q_p was obtained by solving a system of two Eq. 3 with unknown q_p and C:

$$q_p = \frac{T_1/V_1 - T_2/V_2}{C_2 - C_1}$$

With q_p thus determined, intracellular protein concentration is found as

$$C = \frac{T/V}{q_p}$$

when cells are imaged in a low-protein buffer.

Determination of the cell cycle phase. In one experiment, HeLa cells grown on coverslips and mounted on slides as described above were imaged repeatedly at 2.5 h intervals for 25 h. In others, the cycle phase for individual cells was estimated by combination of DNA staining and cell volume, in a manner similar to that used in flow cytometry (Nüsse et al, 1990).

Investigation of the RVI response. HeLa cells were equilibrated in DMEM with 7 mg/ml AB9 (360 mOsm) for 15-20 min, whereupon they were transferred into DMEM containing additionally 40 mM NaCl. We used NaCl rather than the more common mannitol or sucrose in order to avoid changing the refractive index of the medium. For incubations lasting 1 h or less, the cells were kept between a coverslip and a slide; for 20 h time points, the hyperosmotic medium was added to a cell culture dish containing a coverslip with attached cells.

Statistical analysis. The analysis was performed by IBM SPSS 22. When groups of cells were analyzed together, the statistical significance was determined by ANCOVA.

<center>**Results**</center>

TIE calibration. **Fig. 1** shows brightfield, TIE and TTD images of cells in a protein-free buffer and with BSA. The main difference between brightfield images is the visibility of cell boundaries. Accordingly, TIE images show reduced or inverted intensities in BSA compared to those without BSA. By analyzing 72 cells from 4 experiments, the value of q_P was measured as 1.02 (SD = 0.2) in units of rad*ml/μm^3*g or rad/pg.
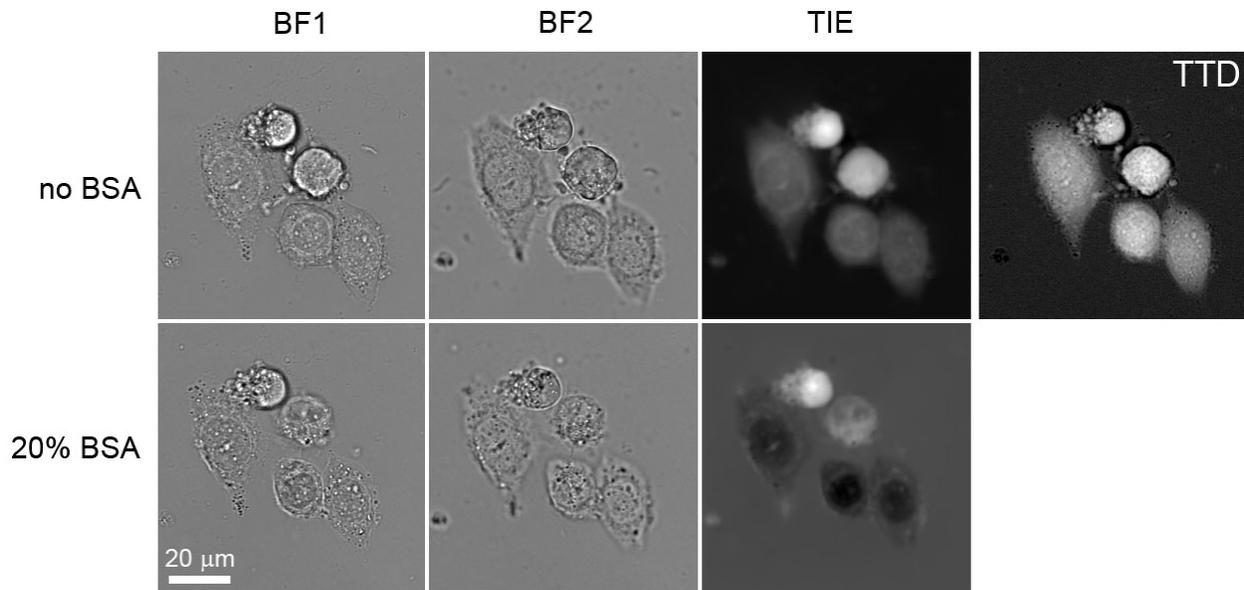

Figure 1. Generation of TIE images. The field shows three HeLa cells with normal morphology and two apoptotic dehydrated cells. The two brightfield images BF1 and BF2 separated vertically by 5 μm were acquired first in a protein-free buffer and then in a buffer containing 20% BSA. The TIE image in the absence of external protein shows all cells as brighter than the background; note the slightly darker nuclei due to their lower refractive index (Liu et al, 2016). In the presence of BSA, the apoptotic cells are still brighter than the background (reflecting the fact that their refractive index is higher than that of

20% BSA), but the contrast is inversed for unaffected cells. From the difference in the TIE contrast with and without BSA, the calibration factor was calculated, as described in the text. A separate panel shows a TTD image, in which the local brightness is proportional to cell thickness.

No difference in q_p was noted between rounded mitotic and spread interphase HeLa cells. To test further whether the results are sensitive to cell shape, we prepared deformed and sometimes dehydrated apoptotic cells by overnight treatment with actinomycin D (Kasim et al, 2013). The value of q_p obtained in that experiment, was 1.15 (SD = 0.13, n = 34) for apoptotic and 1.15 (SD = 0.1, n = 6) for cells with normal morphology. For practical purposes, intracellular protein concentration can be estimated from a TTD image in a low-protein buffer as

$$C(g/ml) \approx 1.0 \cdot T(rad)/V(\mu m^3)$$

Stability of protein concentration throughout the cell cycle. The question of stability of protein/water content was addressed in two types of experiments. In one experiment, HeLa cells were observed every 2.5 hours during 25 hours while kept under a coverslip in DMEM/AB9. Cells kept growing at approximate rate 4% per hour (no attempt was made to characterize their growth in more detail). The time of division was estimated to within half the observation interval. The results of protein measurements are displayed in **Fig. 2A**. While a slight increase in protein concentration was noted around the time of cell division and shortly thereafter, the difference was slight. Based on all data points analyzed, the average protein concentration was 0.194 g/ml (SD = 0.018, n = 116).
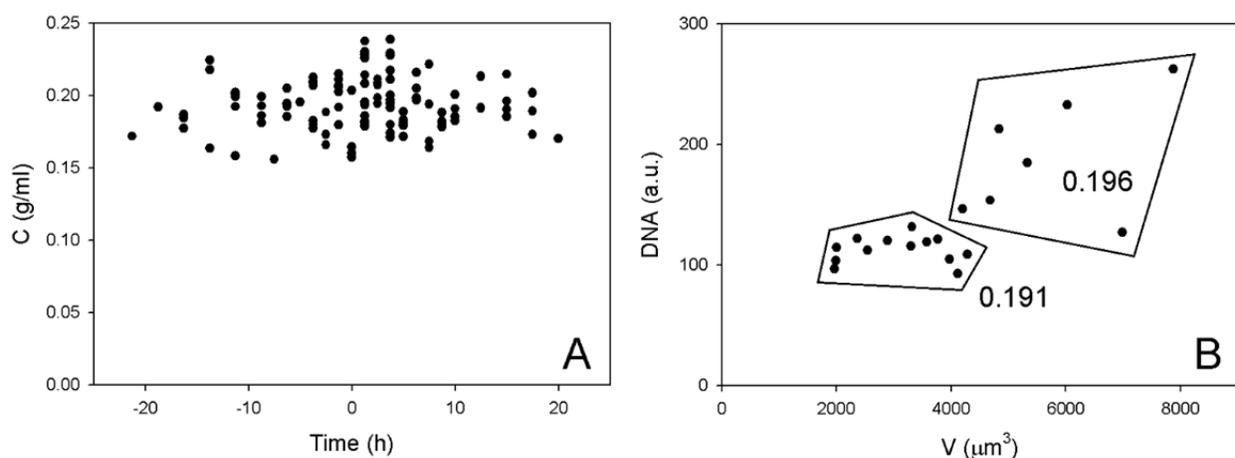

Figure 2. (A) Intracellular protein concentration in HeLa cells before (t < 0), during (t = 0), and after (t > 0) cell division. (B). An example of scatter-plot analysis of DU145 cells. Two groups were identified based on their Hoechst staining and volume; the average protein concentration (g/ml) is indicated for each group.

Observation of MDCK and DU145 cells by this method proved problematic: MDCK cells were extremely labile and continuously kept changing their positions and shapes, making it difficult to relate the images taken at different times, while DU145 cells poorly tolerated prolonged incubation under a coverslip. Therefore, both fluorescence and TTD images of these cells were taken at a single time point, and the cells were divided into two groups: with low DNA/low volume and with high DNA/high volume (**Fig. 2B**). The average values of C (low/high) were 0.191/0.196 and 0.182/0.179 in two experiments with DU145 cells and 0.200/0.184 and 0.184/0.186 with MDCK cells (because of variability of Hoechst staining, the

scatter plots from different experiments cannot be overlaid). Thus, there was no consistent difference between protein concentrations at the early and late stages of the cycle. Plotting of C against volume or DNA individually did not reveal any significant correlation either (not shown).

Example of TTD/TIE: Investigation of Regulatory Volume Increase (RVI). Many cell types have the ability to recover their original volume after initial swelling or shrinkage in a medium with different osmolarity. HeLa cells exhibit rapid RVD in a hyposmotic medium (not shown) but no RVI during the first hour in a hyperosmotic medium (**Fig. 3)**. However, the average protein concentration does return to its original value after a longer incubation of 20 h; thus, a slow RVI still takes place in these cells.
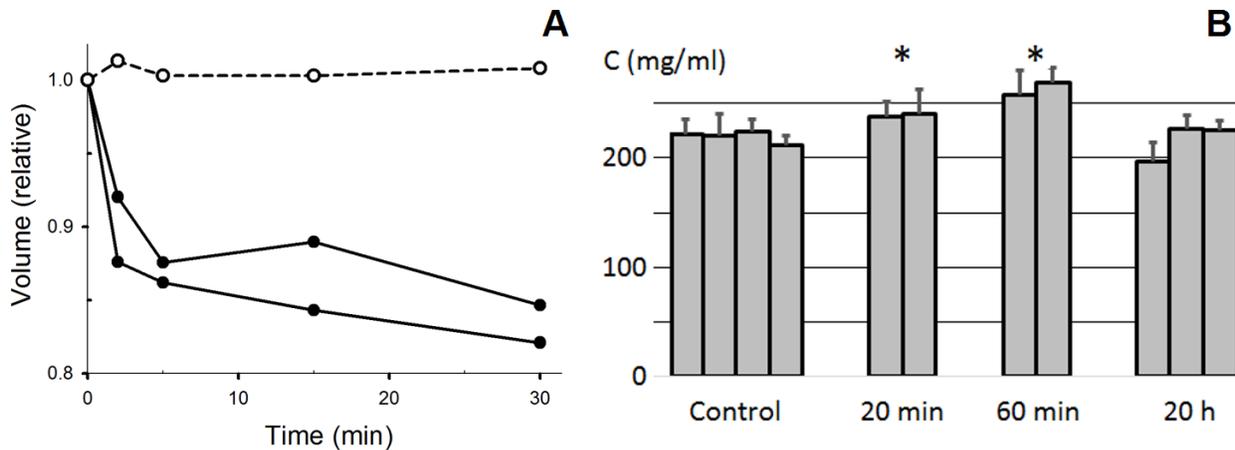
Figure 3. (A). Volume changes in HeLa cells following replacement of a 360 mOsm medium (DMEM with AB9) with a 440 mOsm medium. Solid lines show the results of two separate experiments, and the broken line is a control. Same cells or groups of cells were measured at different time points in these experiments (B). Protein concentration following a transition to the 440 mOsm medium. Each bar represents a separate experiment. Asterisks indicate a significant difference (p<0.001) with the control; protein concentration after a 20 h incubation was not statistically different from the control.

Discussion

In discussions of cell volume regulation, it is often stated that a cell can be characterized by its "natural" volume determined by some intrinsic set point. Although this may be true for stable and differentiated tissues and organs, it obviously does not apply to actively dividing cell populations, where the cell volume doubles between divisions. The point is perhaps merely semantic but reflects the tendency to think in terms of the volume. We believe that, in some cases, it would be more natural to consider protein or water concentration rather than for the volume. However, to make such a change of language meaningful, one has to have a means of measuring the protein concentration in individual cells. Thus we sought to adapt a quantitative phase technique to achieve an accurate and reliable measurement of intracellular protein.

Although quantitative phase imaging underwent significant development in the last two-three decades (Popescu, 2011), it often requires expensive equipment, such as optical tomography, or custom-built optical setups. TIE, on the other hand, can be realized in almost any laboratory, and MATLAB codes for image processing are available (for example, it can be downloaded from http://www.laurawaller.com/ or from Phillips et al (2014)).

In the present work, we adopted a semiempirical approach to TIE, combining the numerical solution of the equation with an experimentally determined parameter. Its justification lies in the fact that TIE produces, beyond doubt, qualitatively correct results, such as reduced water content in apoptotic cells, increased water content within necrotic blebs and preservation of the phase during osmotic swelling or shrinkage (Model and Schonbrun, 2013). However, in all our recent attempts to apply TIE either to cells or to plastic microspheres, the measured phase delay was significantly smaller than expected. Similar results were obtained using a different TIE code from Dr. L. Waller's lab. This lead us to believe that our earlier success in measuring water content in HeLa cells at the expected 85% was by accident. This time, we have thoroughly tested the vertical drive on our microscope and found no evidence of error. But even more importantly, the present method of BSA-based calibration does not even rely on the accuracy of the vertical stage movement.

The calibration factor was found to be close to 1.0 rad*ml/μm^3*g with the coefficient of variation CV ≈ 0.2. The relatively large magnitude of the latter may be partly due to the sensitivity of TIE to noise and to the immediate environment of the particular cell, with neighboring cells affecting the background in their vicinity. It is possible that reproducibility can be improved by using more advanced algorithms for solving TIE, which is known to be sensitive to noise, experimental conditions and method of solution (Froustey et al, 2014; Jingshan et al, 2014; Martinez-Carranza et al, 2013; Mitome et al, 2010; Zuo et al, 2014). However, it seems that reproducibility of our measurements was comparable to what is achieved by many other quantitative phase techniques (Liu et al, 2016).

Our measurements on healthy HeLa cells gave the intracellular protein concentration of 0.2 g/ml on average, which is similar to previously published numbers (Beall et al, 1976). To convert protein concentration into water content (as percent of the total volume), we measured volume expansion upon dissolving BSA in water (not shown) and arrived at the relationship

$$W = 1 - 0.73[BSA]$$

where BSA concentration is expressed in g/ml. Thus, when intracellular water is measured in a low-protein buffer, the appropriate formula for W would be:

$$W \approx 1 - 0.73(T/V)$$

or, in terms of Eq. (4),

$$q_w = 1.37q_p \approx 1.4 \text{ rad}/\mu m^3$$

It follows that the intracellular protein concentration of 0.2 g/ml in HeLa cells corresponds to 85% water.

Although the described calibration procedure is essentially based on refractive index differences, it skips the explicit step of refractive index determination. However, the parameter q_n (see Eq. 5) can be estimated from the refractive index increment dn/dC, which is 0.19-0.20 (ml/g) for BSA solutions 9 Theisen et al, 2000). Therefore, by substituting $0.2C = n - n_o$ into Eq. 3 we find

$$q_n = 5q_p \approx 5 \text{ rad}/\mu m^3$$

For comparison, the value of q'_n obtained directly from TIE under the standard assumption T = φ (phase delay) and for λ = 485 nm would be

$$q_n' = 2\pi/\lambda = 12.3 \text{ rad/}\mu m^3$$

Thus, the empirical coefficient differs from the theoretical result by a factor of 2.5. This is roughly equal to the magnitude of mismatch that can be inferred from other published data (Zhang et al, 2015). Our own measurements with beads have also underestimated the vertical bead size by approximately twofold (not shown). Beads, however, are complex objects that generate multiple reflections and refractions at large angles, which are not accounted for by the TIE theory.

Our results for q_p were reproducible enough (CV ≈ 0.1), and, what is especially encouraging, the same value for the coefficient sufficiently well describes deformed and dehydrated apoptotic cells with higher refractive index. That means that TIE is suitable to study apoptotic volume loss and, in particular, to resolve the above-mentioned dilemma of dehydration vs. fragmentation. Apoptotic dehydration often causes a 50% or larger increase in protein concentration and is easily distinguishable from normal cell variability or scatter in the data.

Having established that BSA-based calibration yields consistent and reasonable numbers, we asked whether water/protein concentration is preserved throughout the cell cycle. This is an important point for interpretation of results on growing and dividing cells, especially when observation has to be carried out for sufficiently long periods. Previous measurements on mammalian cells have shown that monkey kidney CV-1 cells have the highest density at the beginning of G1 phase (Zucker et al, 1979), but the densities of CHO (Anderson et al, 1970) and three mouse cell lines (Loken and Kubitschek, 1984) remain constant; HeLa cells were found to have the lowest protein concentration during mitosis (Beall et al, 1976), which is clearly at odds with our results. However, measurements on yeast have also produced conflicting results in the past (Bryan et al, 2010). Apparently, there is no universal law governing the balance between cell metabolism and water regulation during the cell cycle, and each cell line under given conditions may have to be tested separately.

As an illustration of the importance of protein concentration, we examined the long-term cell volume adaptation in HeLa cells placed in a hyperosmotic buffer. In agreement with previous studies (Barros, 1999; Tivey et al, 1985), we found no sign of RVI during the first 30-60 min (while the cell volume can be directly compared to the initial volume). However, after 20 h, cell protein concentration returned to the same levels as in the isosmotic buffer. This observation is not totally unexpected in itself because different mechanisms may operate during the early and late stages of RVI (Burg et al, 2007); however, the point is that this result would be difficult to obtain from volume measurements alone, as any RVI would be concealed by the normal volume changes that occur during the cell cycle.

Cell volumes can be effectively measured on suspended cells by the electronic sizing technique. However, cell capacity for regulatory volume change depends on their state of attachment: only suspended, but not adherent, HeLa cells are known to exhibit RVI (Barros, 1999; Tivey et al, 1985; Wehner et al, 2007). Thus, if one is interested in the behavior of adherent cells, they should be analyzed without disrupting their attachment. But analyzing enough cells in microscopic images to get good volume statistics may be difficult, especially since partial local cell synchronization is possible. Protein concentration is a much more telling parameter, and analysis of only a small number of cells can produce statistically meaningful data.

Measuring protein concentration may also be more logical in prolonged experiments. Indeed, there are three main factors that are presumed to serve as volume sensors: mechanical tension, concentration of

ions and macromolecular crowding. It is difficult to envision how mechanical stretch or compression can persist over the course of many hours in growing and mobile cells. Ion concentrations are expected to remain more or less stable throughout isosmotic volume changes and can hardly guide the cell towards the set point (although preservation of ion concentration is not supported by all data (Emma et al, 1997). However, the degree of macromolecular crowding, which can affect numerous cellular reactions (Ellis, 2001), could easily act as a persistent signal indicating deviation from the normal structure. In this case, protein concentration is not only a convenient, but a biologically relevant parameter.

Conclusion. The combination of calibrated TIE and TTD can be a practical and powerful tool for studying intracellular water accumulation, cell growth, and related processes. It can be realized at no or minimal cost in any laboratory equipped with a standard microscope.

Literature

Anderson EC, Petersen DF &Tobey RA (1970). Density invariance of cultured Chinese hamster cells with stage of the mitotic cycle. Biophys J 10, 630–645.

Arvill A, Johansson B & Jonsson O (1969). Effects of hyperosmolarity on the volume of vascular smooth muscle cells and the relation between cell volume and muscle activity. Acta Physiol Scand 75, 484-95.

Barone-Nugent ED, Barty A & Nugent KA (2002). Quantitative phase-amplitude microscopy I: optical microscopy. J Microsc 206, 194-203.

Barros LF (1999). Measurement of sugar transport in single living cells. Pflugers Arch 437, 763-770.

Beall PT, Hazlewood CF & Rao PN (1976). Nuclear magnetic resonance patterns of intracellular water as a function of HeLa cell cycle. Science 192, 904-907.

Bryan AK, Goranov A, Amon A & Manalis SR (2010). Measurement of mass, density, and volume during the cell cycle of yeast. Proc Natl Acad Sci U S A 107, 999-1004.

Burg MB, Ferraris JD & Dmitrieva NI (2007). Cellular response to hyperosmotic stress. Physiol Rev 87, 1441–1474.

Carlsson K (1991). The influence of specimen refractive index, detector signal integration, and non-uniform scan speed on the imaging properties in confocal microscopy. J Microsc 163, 167–178.

Curl CL, Bellair CJ, Harris T, Allman BE, Harris PJ, Stewart AG, Roberts A, Nugent KA & Delbridge LM (2005). Refractive index measurement in viable cells using quantitative phase-amplitude microscopy and confocal microscopy. Cytometry A 65, 88-92.

Ellis RJ (2001). Macromolecular crowding: obvious but underappreciated. Trends Biochem Sci 26, 597-604.

Emma F, McManus M & Strange K (1997). Intracellular electrolytes regulate the volume set point of the organic osmolyte/anion channel VSOAC. Am J Physiol 272, C1766-1775.

Fulton AB (1982). How crowded is the cytoplasm? Cell 30, 345-347.

Froustey E, Bostan E, Lefkimmiatis S & Unser M (2014) Digital phase reconstruction via iterative solutions of transport-of-intensity equation. Information Optics (WIO), 13th Workshop, pp 1-3.

Gorthi SS & Schonbrun E (2012). Phase imaging flow cytometry using a focus-stack collecting microscope. Opt Lett 37, 707-709.

Gregg JL, McGuire KM, Focht DC & Model MA (2010). Measurement of the thickness and volume of adherent cells using transmission-through-dye microscopy. Pflugers Arch 460, 1097-1104.

Heijnen JJ (2010). Growth nutrients and diversity. In The Metabolic Pathway Engineering Handbook: Fundamentals, ed. Smolke C, pp 6.1 – 6.9. CRC Press, Boca Raton, FL.

Hoffmann EK, Lambert IH & Pedersen SF (2009). Physiology of cell volume regulation in vertebrates. Physiol Rev 89, 193-277.

Ishizuka K & Allman B (2005). Phase measurement in electron microscopy using the transport of intensity equation. Microscopy Today 13, 22-24.

Jingshan Z, Claus RA, Dauwels J, Tian L & Waller L (2014). Transport of Intensity phase imaging by intensity spectrum fitting of exponentially spaced defocus planes. Opt Express 22, 10661-10674.

Jones AW (1982). Electrolyte metabolisms of the arterial wall. In Vascular Smooth Muscle: Metabolic, Ionic, and Contractile Mechanisms, ed. Crass MF III & Barnes CD, pp 37-70. Academic Press, New York.

Kasim NR, Kuželová K, Holoubek A & Model MA (2013). Live fluorescence and transmission-through-dye microscopic study of actinomycin D-induced apoptosis and apoptotic volume decrease. Apoptosis 18, 521-532.

Liu PY, Chin LK, Ser W, Chen HF, Hsieh CM, Lee CH, Sung KB, Ayi TC, Yap PH, Liedberg B, Wang K, Bourouina T & Leprince-Wang Y (2016). Cell refractive index for cell biology and disease diagnosis: past, present and future. Lab Chip 16, 634-644.

Loken MR & Kubitschek HE (1984). Constancy of cell buoyant density for cultured murine cells. J Cell Physiol 118, 22–26.

Martinez-Carranza J, Falaggis K, Kozacki T & Kujawinska M (2013). Effect of imposed boundary conditions on the accuracy of transport of intensity equation based solvers. Proc SPIE 8789, 87890N-87890N-14

Mitome M, Ishizuka K & Bando Y (2010). Quantitativeness of phase measurement by transport of intensity equation. J Electron Microsc (Tokyo) 59, 33-41.

Model MA (2012). Imaging the cell's third dimension. Microscopy Today 20, 32-37.

Model MA (2014). Intensity calibration and flat-field correction for fluorescence microscopes. Curr Protoc Cytom 68, 10.14.1-10.14.10.

Model MA (2015). Cell volume measurements by optical transmission microscopy. Curr Protoc Cytom 72, 12.39.1-12.39.9.

Model MA & Burkhardt JK (2001). A standard for calibration and shading correction in fluorescence microscopy. Cytometry 44, 309-316.

Model MA, Khitrin AK & Blank JL (2008). Measurement of the absorption of concentrated dyes and their use for quantitative imaging of surface topography. J Microsc 231, 156-167.

Model MA & Schonbrun E (2013). Optical determination of intracellular water in apoptotic cells. J Physiol 591, 5843-6849.

Nüsse M, Beisker W, Hoffmann C & Tarnok A (1990). Flow cytometric analysis of G1- and G2/M-phase subpopulations in mammalian cell nuclei using side scatter and DNA content measurements. Cytometry 11, 813-21.

Phillips KG, Jacques SL & McCarty OJ (2012). Measurement of single cell refractive index, dry mass, volume, and density using a transillumination microscope. Phys Rev Lett 109, 118105.

Phillips KG, Baker-Groberg SM & McCarty OJ (2014). Quantitative optical microscopy: measurement of cellular biophysical features with a standard optical microscope. J Vis Exp 86 doi: 10.3791/50988.

Popescu G (2011). Quantitative Phase Imaging of Cells and Tissues. McGraw-Hill, New York.

Rao PN, Hazlewood CF & Beall PT (1982). Cell cycle phase-specific changes in relaxation times and water content in HeLa cells. In Cell Growth, ed. Nicolini C, pp 535-548. Plenum Press, New York.

Theisen A, Johann C, Deacon MP & Harding SE (2000). Refractive Increment Data-Book for Polymer and Biomolecular Scientists. Nottingham University Press, Nottingham.

Tivey DR, Simmons NL & Aiton JF (1985). Role of passive potassium fluxes in cell volume regulation in cultured HeLa cells. J Membr Biol 87, 93–105.

Visser TD, Oud JL & Brakenhoff GJ (1992). Refractive index and axial distance measurements in 3-D microscopy. Optik 90, 17–19.

Wehner F, Numata T, Subramanyan M, Takahashi N & Okada Y (2007). Signalling events employed in the hypertonic activation of cation channels in HeLa cells. Cell Physiol Biochem 20, 75-82.

Zhang Z, Chen W & Barbastathis G (2015). Phase imaging using a hybrid approach: combining wavefront sensing with the transport-of-intensity equation. In Digital Holography & 3-D Imaging Meeting, OSA Technical Digest (Optical Society of America, 2015), paper DT1A.5.

Zhao H, Brown PH & Schuck P (2011). On the distribution of protein refractive index increments. Biophys J 100, 2309–2317.

Zucker RM, D'Alisa RM & Gershey EL (1979). Characterization of a CV-1 cell cycle. III. Biophysical parameters. Exp Cell Res 122, 1-8.

Zuo C, Chen Q & Asundi A (2014). Boundary-artifact-free phase retrieval with the transport of intensity equation: fast solution with use of discrete cosine transform. Opt Express 22, 9220-9244.
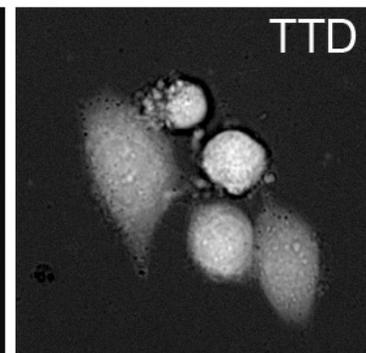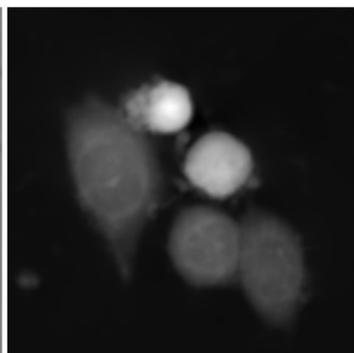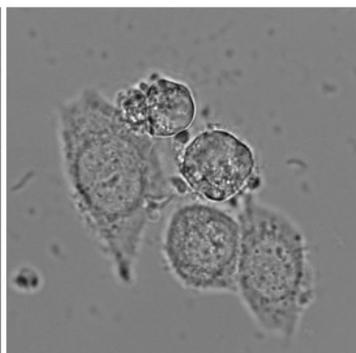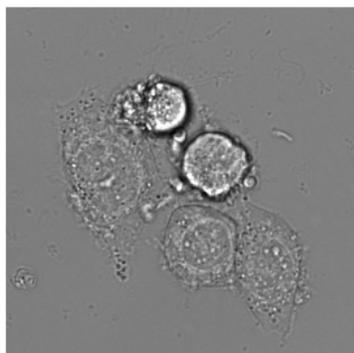
	BF1	BF2	TIE	TTD
no BSA				
20% BSA				

20 μm